Liquid Crystals
Publication details, including instructions for authors and subscription information:
http://www.informaworld.com/smpp/title~content=t713926090

The magnetic field-induced deformations in nematic layers with non-zero splay-bend elastic constant

Grzegorz Derfel[a]
[a] Technical University of Łódź, Institute of Physics, Łódź, Poland

To cite this Article Derfel, Grzegorz(1996) 'The magnetic field-induced deformations in nematic layers with non-zero splay-bend elastic constant', Liquid Crystals, 21: 6, 791 — 799
To link to this Article: DOI: 10.1080/02678299608032895
URL: http://dx.doi.org/10.1080/02678299608032895

LIQUID CRYSTALS, 1996, VOL. 21, NO. 6, 791–799

The magnetic field-induced deformations in nematic layers with non-zero splay-bend elastic constant

by GRZEGORZ DERFEL
Technical University of Łódź, Institute of Physics, ul. Wólczańska 223, 93-005 Łódź, Poland

(*Received 14 July 1995; in final form 22 February 1996; accepted 7 July 1996*)

The magnetic field-induced deformations of weakly anchored nematic layers in the presence of the non-zero splay-bend elastic constant k_{13} are analysed by use of the Pergamenshchik approach. Most of the anomalous phenomena reported by other authors, that do not occur if $k_{13} = 0$, have been confirmed. New effects suitable for experimental verification are predicted: the discontinuous transition with hysteresis between the uniform undistorted state and the state uniformly aligned along the field, and the rotation of the director in the tilted layer during continuous increase and decrease of the perpendicular field.

1. Introduction

The splay-bend term, which was reinstated into the Frank elastic free energy density of the nematic liquid crystal by Nehring and Saupe [1], causes well known problems [2, 3]. The functional of the total free energy including this term has no minimum, so the director distribution cannot be found by means of the variational method. The problem was referred to as the 'ill-posed', and two different approaches which allow one to by-pass the mathematical difficulties have been proposed. Barbero *et al.* [4] generalized the Frank theory of elasticity by addition of a term of the fourth order in the director derivatives. As a result, the free energy functional possesses a minimum. This approach is referred to as the 'second order' elastic theory. It is rather troublesome for practical use, since 35 new elastic constants are required for the full expression of the second order free energy density. The approximate approach with only one bulk second order elastic constant predicts extremely strong sub-surface distortions which cause some other problems [3]. According to the other approach, proposed by Pergamenshchik [2], the director distribution should be searched in the class of continuous solutions of the Euler–Lagrange equation related to the first order elastic free energy, i.e. to the Frank expression. Several proposals for the experimental verification of these two theories have been made [3, 5]. The situations, for which both theories predict the qualitatively different behaviours, not simply quantitatively different results, would be especially worthy of experimental examination. The effects predicted by the second order theory should take place on the molecular scale length and are practically inaccessible to standard experimental methods. Any experiment would give results which could be interpreted, without any surface-like elastic constants, by the use of suitably fitted anchoring energy and surface alignment direction. On the other hand, some spectacular unexpected effects were predicted on the basis of the first order approach. They concern a weakly anchored nematic layer deformed by a magnetic field. (The angle θ mentioned below describes the director distribution in the layer. It depends on the coordinate z measured perpendicular to the layer plane.)

(i) Spontaneous deformation can take place in the absence of the field [6].
(ii) Under the action of the field, the spontaneous deformation transforms into the anomalous structure described by the odd $\theta(z)$ function and is finally suppressed [6].
(iii) The usual deformation, described by the even $\theta(z)$ function, can be suppressed by an increasing field [6].
(iv) The magnetic field directed parallel to the easy axis deforms the director distribution [3].
(v) The orientation of the director adjacent to the boundary surfaces remains unperturbed, in spite of the action of the field, only if the field vector makes some special angle with the surface easy axis [3].

In the present paper, the behaviour of the nematic liquid crystal in the magnetic field is reanalysed in terms of the Pergamenshchik approach. The effects mentioned above were confirmed, with the exception of (iii) and

0267–8292/96 $12·00

(v). Some other anomalous features of behaviour were found:

(vi) Deformation in the magnetic field perpendicular to the tilted easy axis arises without threshold.

(vii) Discontinuous transition with hysteresis occurs between the undeformed state and the structure totally aligned along the field.

(viii) The director rotates during repeated increases and decreases of the field.

(ix) The asymmetric deformations are typical for arbitrary field directions and surface orientations.

Experimental evidence for these effects would confirm the Pergamenshchik theory, whereas the absence of these effects could be interpreted as favouring the second order theory.

In §2 of this paper, the assumptions concerning the system are precisely stated, and the method of analysis is described. Section 3 presents the results. The conditions leading to spontaneous deformation in the absence of the field are found, and threshold type deformations occurring in special cases are described. The variety of effects taking place in some particular geometries are also exemplified. The results are summarized and discussed in §4.

2. Assumptions and method

The nematic liquid crystal, characterized by elastic constants $k_{33} = k_{11} = k$, $k_{sb} = k_{13}/k$ and by a small positive diamagnetic anisotropy $\Delta\chi$, is confined between two plates positioned at $z = \pm d/2$ parallel to the xy plane as shown in figure 1. The director $\mathbf{n}$ lies in the yz plane and makes an angle $\theta(z)$ with the z axis. The surface anchoring energy is finite and described by the Rapini–Papoular formula

$$F_{\text{anchoring}} = \gamma[\sin^2(\theta_1 - \beta) + \sin^2(\theta_2 - \beta)] \qquad (1)$$

where γ measures the energy of the surface interaction per unit area, $\theta_1 = \theta(-d/2)$, $\theta_2 = \theta(+d/2)$ and β is the angle between the easy axis of the surface alignment $\mathbf{e}$ and the z axis. The bias magnetic field of strength $\mathbf{H}$ lies in the yz plane and makes the angle α with the y axis.

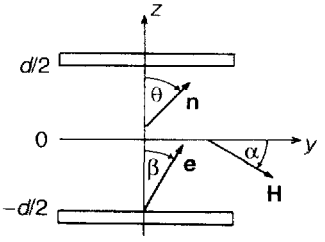

Figure 1. The geometry of the system.

The total free energy per unit area of the layer is expressed by:

$$F = \frac{1}{2}\int_{-d/2}^{d/2}\left[k\left(\frac{d\theta}{dz}\right)^2 - \Delta\chi\mathbf{H}^2\sin^2(\theta-\alpha)\right]dz + \gamma[\sin^2(\theta_1-\beta)+\sin^2(\theta_2-\beta)] - \frac{1}{2}k_{13}\left[\frac{d\theta}{dz}\left(\frac{d}{2}\right)\sin 2\theta_2 - \frac{d\theta}{dz}\left(-\frac{d}{2}\right)\sin 2\theta_1\right] \qquad (2)$$

After some substitutions and abbreviations:

$$h = \mathbf{H}/H_c, \quad H_c = \frac{\pi}{d}(k\Delta\chi)^{1/2}, \quad u = \pi h\zeta, \quad \zeta = z/d$$
$$U = \pi h/2, \quad \delta = \theta - \alpha, \quad \delta'_u = d\delta/du, \quad g = \gamma d/k, \qquad (3)$$

this expression takes the form:

$$F = \frac{k}{d}\left\{U\int_{-U}^{U}[\delta'^2_u - \sin^2\delta]du + g[\sin^2(\delta_1+\alpha-\beta)+\sin^2(\delta_2+\alpha-\beta)] - k_{sb}U[\delta'_{u,2}\sin 2(\delta_2+\alpha) - \delta'_{u,1}\sin 2(\delta_2+\alpha)]\right\} \qquad (4)$$

where the indices 1 and 2 refer to $z = -d/2$ and to $z = d/2$, respectively. According to the Pergamenshchik approach, the director distribution function $\delta(u)$ should be searched in the class of the continuous functions which satisfy the Euler–Lagrange equation applied to the Frank part of the free energy. The parameters which specify the director distribution, i.e. the particular values of the integration constants, are calculated by minimization of the free energy function F obtained when $\delta(u)$ is substituted into the expression (4). Various k_{sb} values were used during the numerical computations, since the experimental [7, 8] and theoretical [1, 9, 10] estimations are widely scattered.

3. Results

By use of the substitution $\delta = \theta - \alpha$, the Euler–Lagrange equation writes:

$$\frac{d^2\delta}{du^2} + \sin\delta\cos\delta = 0 \qquad (5)$$

The general solution of this equation is

$$\delta = \arcsin\{[\mathrm{sn}(u-u_0,c)\cos(\beta-\alpha)(c^2-\sin^2(\beta-\alpha))^{1/2} + \sin(\beta-\alpha)\,\mathrm{cn}(u-u_0,c)\,\mathrm{dn}(u-u_0,c)] \times [1-\sin^2(\beta-\alpha)\,\mathrm{sn}^2(u-u_0,c)]^{-1}\} \qquad (6)$$

for $c \leqslant 1$, and

$$\delta = \arcsin\left\{\left[\operatorname{sn}\left(c(u-u_0),\frac{1}{c}\right)\right.\right.$$
$$\times \cos(\beta-\alpha)\left(1-\frac{1}{c^2}\sin^2(\beta-\alpha)\right)^{1/2}$$
$$\left.+\sin(\beta-\alpha)\operatorname{cn}\left(c(u-u_0),\frac{1}{c}\right)\operatorname{dn}\left(c(u-u_0),\frac{1}{c}\right)\right]$$
$$\left.\times\left[1-\frac{1}{c^2}\sin^2(\beta-\alpha)\operatorname{sn}^2\left(c(u-u_0),\frac{1}{c}\right)\right]^{-1}\right\} \quad (7)$$

for $c \geqslant 1$. In (6) and (7), cn, dn and sn are the elliptic Jacobian functions [11], whereas c and u_0 denote the integration constants. Their physical meaning is as follows:

$$u_0 = \pi h \zeta_0 \quad (8)$$

where ζ_0 is the reduced coordinate for which $\theta = \beta$, i.e. $\delta = \beta - \alpha$, and

$$c^2 = \delta_u'^2(u_0) + \sin^2(\alpha - \beta) \quad (9)$$

If $c \leqslant 1$, it can be identified with

$$c = \sin \delta_m, \quad (10)$$

where δ_m is the extreme value of δ. (The details of integration are given in the Appendix.) In general, the solutions (6) and (7) represent the fully asymmetric distribution. However, in special cases, the $\delta(u)$ functions are even or odd, describing symmetric or antisymmetric director distributions, respectively.

3.1. *Zero-field director distribution*

In the absence of the field, the quantity $u - u_0$ equals zero. Two types of zero-field director distributions are possible. The solution (6) gives $\delta = \beta - \alpha$, i.e. $\theta = \beta$, since $\operatorname{sn}(0, c) = 0$ and $\operatorname{cn}(0, c) = \operatorname{dn}(0, c) = 1$. The director distribution is uniform and parallel to the surface easy axis. Equation (7) gives a solution of a different type, provided that c tends to infinity, assuring that $c(u - u_0) = \rho(\zeta - \zeta_0)$ remains finite when h tends to zero:

$$\delta = \rho(\zeta - \zeta_0) + \beta - \alpha \quad (11)$$

or

$$\theta = \rho(\zeta - \zeta_0) + \beta \quad (12)$$

where the following properties of the Jacobian functions were used: $\operatorname{sn}(u - u_0, 0) = \sin(u - u_0)$, $\operatorname{cn}(u - u_0, 0) = \cos(u - u_0)$ and $\operatorname{dn}(u - u_0, 0) = 1$. The quantity $\rho = \pi hc$ tends to $\delta_\zeta'(\zeta_0)$ in this limit. The linear $\theta(\zeta)$ dependence is consistent with the solution of the zero-field Euler–Lagrange equation

$$\frac{d^2\theta}{dz^2} = 0 \quad (13)$$

With application of the formula (11), the expression for the free energy (4) reduces to

$$F = \frac{k}{d}\left\{\frac{\rho^2}{2} + g\left[\sin^2\left(\rho\left(\frac{1}{2}+\zeta_0\right)\right) + \sin^2\left(\rho\left(\frac{1}{2}-\zeta_0\right)\right)\right]\right.$$
$$\left. - k_{sb}\rho \sin\rho\cos 2(\beta - \rho\zeta_0)\right\} \quad (14)$$

If $k_{sb} = 0$, then the value $\rho = 0$ yields the minimum free energy $F = 0$, and θ equals β everywhere. (The ζ_0 value is not specified in such a case.) The minimum existing for $\rho = 0$ changes into the maximum if

$$1 + g - 2k_{sb}\cos 2\beta < 0. \quad (15)$$

This means that if $k_{sb} > (1+g)/2\cos 2\beta$ for $0 \leqslant \beta < \pi/4$ or $k_{sb} < -(1+g)/2\cos 2\beta$ for $\pi/4 < \beta \leqslant \pi/2$, the minimum for $\rho \neq 0$ can appear. The numerically obtained example of such a distorted structure is shown in figure 2.

The structures which develop in the increasing field correspond to one of the two types of solutions mentioned above. The examples of such behaviour are presented below.

3.2. *Deformations in the magnetic field perpendicular to the easy axis*

If $\mathbf{H} \perp \mathbf{e}$, i.e. $\beta - \alpha = 0$, then solutions (6) and (7) reduce to:

$$\delta = \arcsin(c \operatorname{sn}(u - u_0, c)) \quad (16)$$

and

$$\delta = \arcsin(\operatorname{sn}(c(u - u_0), 1/c)) \quad (17)$$

respectively. These functions can represent the symmetric and antisymmetric director distributions. The numerical

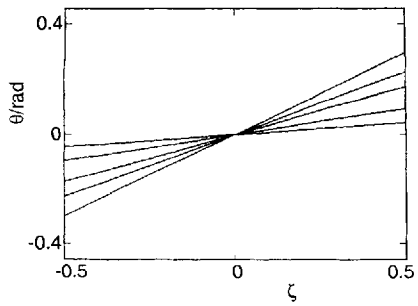

Figure 2. The director distribution in the homeotropic layer ($\beta = 0$) deformed by the field $\mathbf{H} \perp \mathbf{e}$ ($\alpha = 0$) calculated for $k_{sb} = 1{\cdot}1$ and $g = 1$. The values of U are 0, 0·5, 0·6, 0·67 and 0·69 (in order from the highest slope to the lowest).

minimization performed for various parameters proved the existence of each type of solution. The solution which is due to the lower free energy is realized. For $1+g-2k_{sb}\cos 2\beta>0$ only the symmetric solution occurs, and in the opposite case the antisymmetric solution is possible.

The symmetric solution arises if $u_0=\pm K(c)$ is used in equation (16), where $K(c)$ is the real quarter-period of the Jacobian elliptic functions given by the complete elliptic integral of the first kind,

$$K(c)=\int_0^{\pi/2}(1-c^2\sin^2\varphi)^{-1/2}\mathrm{d}\varphi.$$

Due to the properties of the Jacobian functions, the even solution can be written in the form

$$\delta=\arcsin\left(c\frac{\mathrm{cn}(u,c)}{\mathrm{dn}(u,c)}\right) \tag{18}$$

which is identical with the solution given in [12]. Figure 3 presents the symmetric director distribution for several field values. In weakly anchored layers, the intrinsic curvature stiffness of the nematic liquid crystal with small or negative k_{sb} does not allow for strong deformations and the director distribution is relatively flat in comparison to the strong anchoring case.

The antisymmetric solution arises if $u_0=0$ is substituted into (16):

$$\delta=\arcsin(c\,\mathrm{sn}(u,c)) \tag{19}$$

or into (17)

$$\delta=\arcsin(\mathrm{sn}(cu,1/c)) \tag{20}$$

The solution of this kind was predicted in [6]. The examples of the antisymmetric distributions for several field strengths are shown in figure 2. The $\theta(z)$ functions describing them are practically linear

3.2.1. *Threshold-type deformations*

Planar and homeotropic layers, which are uniform in the absence of the field, remain undistorted until the field reaches some threshold strength U_1. Another threshold field, U_2, is the limiting value, above which the layer is uniformly oriented along the field and $\mathbf{n}\|\mathbf{H}$ applies everywhere.

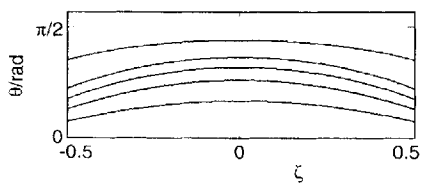

Figure 3. The director distribution in the homeotropic layer ($\beta=0$) deformed by the field $\mathbf{H}\perp\mathbf{e}$ ($\alpha=0$) calculated for $k_{sb}=0{\cdot}1$ and $g=2$. The values of U are 1·2, 1·3, 1·4, 1·5 and 1·7 (in order from the lowest curve to the highest).

If the zero-field structure is linearly deformed (due to the suitable k_{sb} value), then this spontaneous deformation decays gradually under the action of the field and disappears at some threshold magnetic field strength U_3, above which the uniform structure $\mathbf{n}\|\mathbf{e}$ is stable. The relations between all three thresholds depend on the k_{sb} value.

As the values of u_0 are unambiguously defined for the symmetric and antisymmetric solutions considered here, the free energy function, obtained by substitution of a suitable solution (18), (19) or (20) into formula (4), depends only on c. The uniform director distribution, described by $\delta=\beta-\alpha=0$ and determined by equation (18) when $c=0$, satisfies the condition for the extremum of the free energy $\partial F/\partial c|_{c=0}=0$. Therefore its stability is determined by the sign of $\partial^2F/\partial c^2|_{c=0}$. In the following, the homeotropic layer, ($\beta=0$), will be considered.

The undeformed uniform state is stable at low fields since $\partial^2F/\partial c^2|_{c=0}>0$. The threshold U_1 is determined by the equation

$$\partial^2F/\partial c^2|_{c=0}=0 \tag{21}$$

which takes a form

$$(2k_{sb}-1)U_1\sin 2U_1+2g\cos^2U_1=0 \tag{22}$$

It has many solutions determined by

$$U_1=\pi(2n+1)/2\quad\text{where } n=0,\pm1,\pm2,\pm3\ldots \tag{23}$$

and by

$$U_1=\frac{g}{1-2k_{sb}}\cot U_1 \tag{24}$$

but only the lowest positive value obtained for given g and k_{sb} has the sense of the threshold. It is thus given by (24) for $k_{sb}<0{\cdot}5$ and equals $\pi/2$ for $k_{sb}>0{\cdot}5$.

The uniform state, aligned parallel to the field is described by $\delta=\arcsin c=\pi/2$, and is determined by equation (18) when $c=1$. It is useful to analyse its stability by means of $\partial^2F/\partial\delta_m^2$. This state is unstable at sufficiently low fields and becomes stable above the threshold determined by the equation

$$\partial^2F/\partial\delta_m^2|_{\delta_m=\pi/2}=0 \tag{25}$$

which has a form

$$(1+2k_{sb})U_2\sinh U_2-2g\cosh^2U_2=0 \tag{26}$$

or

$$U_2=\frac{g}{1+2k_{sb}}\coth U_2 \tag{27}$$

Equations (24) and (27) are the generalized version of the threshold conditions calculated in [12] for $k_{sb} = 0$.

The linearly deformed zero-field state, existing if $k_{sb} > (1 + g)/2$, decays continuously and transforms into the uniform state $\mathbf{n} \| \mathbf{e}$ above the threshold given by the formula derived from (21)

$$(1 - 2k_{sb})U_3 \sin 2U_3 + 2g \sin^2 U_3 = 0 \qquad (28)$$

or

$$U_3 = -\frac{g}{1 - 2k_{sb}} \tan U_3 \qquad (29)$$

The thresholds obtained from (24), (27) and (29) are plotted in figure 4 as functions of k_{sb} for several values of g. Two relations between U_1 and U_2 are possible. If k_{sb} is sufficiently small or negative then $U_1 < U_2$. The transition between the two uniform states is continuous and has the form shown in figures 5 and 6. For somewhat higher k_{sb}, the transition is discontinuous with hysteresis as shown in figure 7.

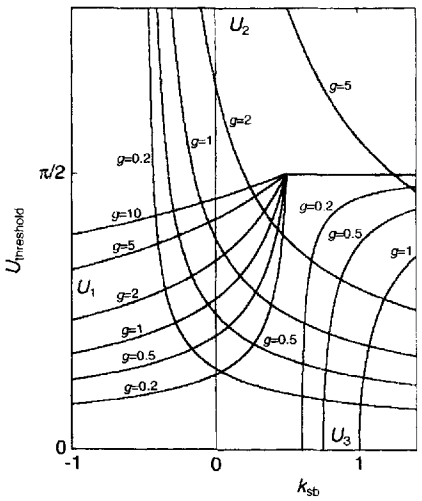

Figure 4. The thresholds U_1, U_2 and U_3 as functions of k_{sb}. The surface anchoring energy parameters g are indicated for each curve.

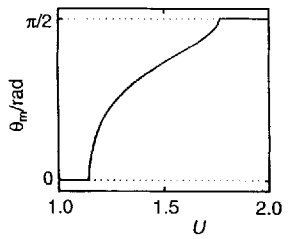

Figure 5. The stationary states of the homeotropic layer ($\beta = 0$) subjected to the magnetic field $\mathbf{H} \perp \mathbf{e}$ ($\alpha = 0$). The mid-plane angle θ_m is plotted as a function of U for $k_{sb} = 0{\cdot}1$ and $g = 2$. The full line denotes the minima of the free energy whereas the dotted lines denote the maxima.

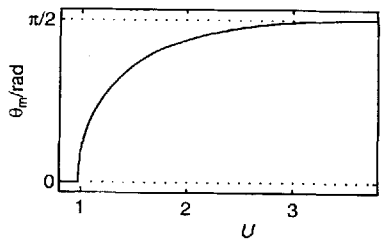

Figure 6. The stationary states of the homeotropic layer ($\beta = 0$) subjected to the magnetic field $\mathbf{H} \perp \mathbf{e}$ ($\alpha = 0$). The mid-plane angle θ_m is plotted as a function of U for $k_{sb} = -0{\cdot}2$ and $g = 1$. The full line denotes the minima of the free energy whereas the dotted lines denote the maxima.

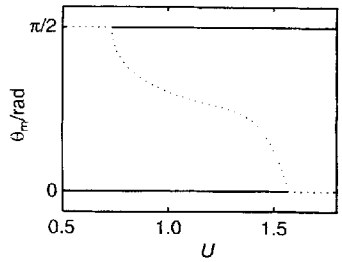

Figure 7. The stationary states of the homeotropic layer ($\beta = 0$) subjected to the magnetic field $\mathbf{H} \perp \mathbf{e}$ ($\alpha = 0$). The mid-plane angle θ_m is plotted as a function of U for $k_{sb} = 0{\cdot}6$ and $g = 1$. The full lines denote the minima of the free energy whereas the dotted line denotes the maxima.

The decay of the spontaneous deformation occurring if the inequality (15) is satisfied, is illustrated in figures 2 and 8. If the field is increased further, then above $U_1 = \pi/2$, the discontinuous transition to the state $\mathbf{n} \| \mathbf{H}$ occurs (not shown in the figures). This state is stable in the decreasing field until the threshold U_2 is reached, below which the layer returns to the linear deformation.

Figure 9 shows the boundary lines separating three regions in the (g, k_{sb}) plane. In the region A, U_1 is lower than U_2, whereas in the regions B and C the opposite relation occurs. The smaller the actual value of k_{sb}, the weaker must be the surface anchoring (or the thinner must be the layer) in order to detect the anomalous

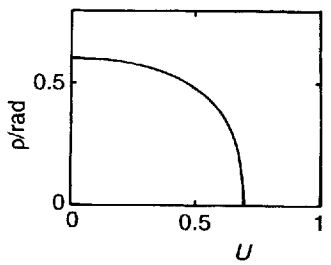

Figure 8. The decay of the linear deformation presented in figure 2. The stationary states are determined by the spatial angle derivative $\rho = \theta'_\zeta|_{\zeta=0}$ plotted as a function of U.

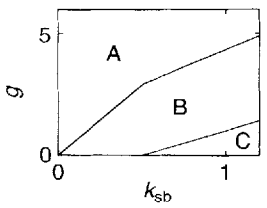

Figure 9. The ranges of k_{sb} and g leading to different properties of the layer. A is the continuous transition between the $\mathbf{n} \| \mathbf{e}$ and $\mathbf{n} \| \mathbf{H}$ states; B is the discontinuous transition with hysteresis; C is the spontaneous deformation in the absence of the field.

hysteresis. In the region C the linear zero-field deformation is possible.

The properties of the planar layers, ($\beta = \pi/2$), are analogous; however the sign before k_{sb} should be changed in the formulae presented above and in the figures mentioned.

3.2.2. *Deformations in oblique fields* $\boldsymbol{H} \perp \boldsymbol{e}$

It is known, that if $k_{sb} = 0$, the deformation has a threshold character for any β, provided $\mathbf{H} \perp \mathbf{e}$ [13, 14]. However if $k_{sb} \neq 0$, the behaviour of the system is different. Figures 10 and 11 show the deformations of the tilted layer with relatively low k_{sb} values subjected to the oblique field $\mathbf{H} \perp \mathbf{e}$. The deformation is thresholdless. The director distribution is symmetrical. An interesting phenomenon can be noticed, namely that rotation of the director takes place if the field is repeatedly increased and decreased, as shown schematically in figure 12.

The case of high k_{sb} values, when the initial linear distribution is deformed, is illustrated in figure 13. The asymmetric distribution decays and transforms gradually

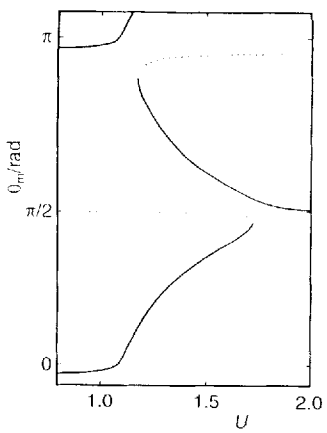

Figure 10. The stationary states of the tilted layer ($\beta = -0{\cdot}1$) subjected to the oblique magnetic field $\mathbf{H} \perp \mathbf{e}$ ($\alpha = -0{\cdot}1$). The mid-plane angle θ_m is plotted as a function of U for $k_{sb} = 0{\cdot}1$ and $g = 2$. Full lines denote the minima of the free energy whereas the dotted lines denote the maxima.

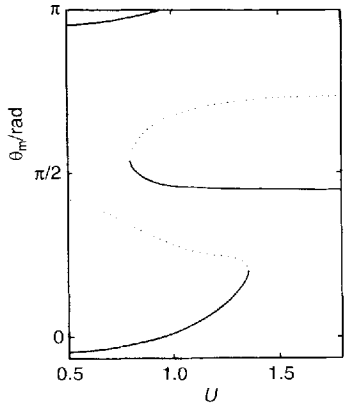

Figure 11. The stationary states of the tilted layer ($\beta = -0{\cdot}2$) subjected to the oblique magnetic field $\mathbf{H} \perp \mathbf{e}$ ($\alpha = -0{\cdot}2$). The mid-plane angle θ_m is plotted as a function of U for $k_{sb} = 0{\cdot}6$ and $g = 1$. Full lines denote the minima of the free energy whereas the dotted lines denote the maxima.

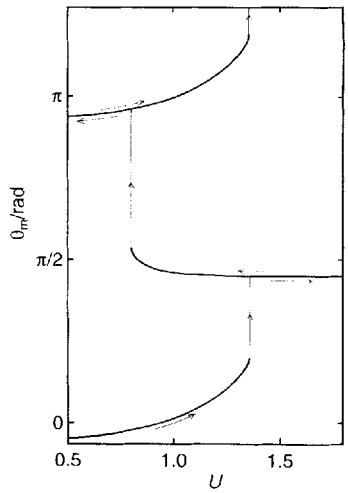

Figure 12. The possibility of director rotation in the tilted layer ($\beta = -0{\cdot}2$) subjected to the repeatedly increasing and decreasing oblique magnetic field $\mathbf{H} \perp \mathbf{e}$ ($\alpha = -0{\cdot}2$). Only the minima of the free energy are shown, $k_{sb} = 0{\cdot}6$ and $g = 1$.

into the symmetric one. The high field deformation has a different character from that shown in figure 3: the layer is strongly distorted, probably due to the high k_{sb} value, which favours director curvature in the boundary regions.

3.3. *Deformations in a parallel field* $\boldsymbol{H} \| \boldsymbol{e}$

If $\mathbf{H} \| \mathbf{e}$, i.e. $\beta - \alpha = \pi/2$, then $c \geqslant 1$, which is evident from equation (9). The solution (7) reduces to

$$\delta = \arcsin \frac{\mathrm{cn}(c(u - u_0), 1/c)}{\mathrm{dn}(c(u - u_0), 1/c)} \tag{30}$$

The field parallel to the surface easy axis does not

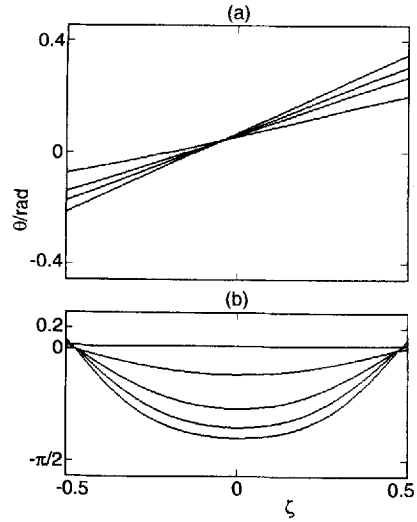

Figure 13. The director distribution in the tilted layer ($\beta = 0{\cdot}1$) deformed by the oblique field $\mathbf{H} \perp \mathbf{e}$ ($\alpha = 0{\cdot}1$) calculated for $k_{sb} = 1{\cdot}1$ and $g = 1$. (*a*) The decay in the asymmetric deformations with increasing field (the values of U are 0·1, 0·4, 0·5 and 0·6, in order from the highest slope to the lowest); (*b*) development of the symmetric deformations with increasing field (the values of U are 0·7, 1·5, 2·0, 2·5 and 3·0, in order from the highest curve to the lowest.

induce any deformation if the inequality (15) is not satisfied. In the opposite case, the initial linear distribution is distorted as shown in figure 14. The surface director deviates from **e** even in high fields, whereas the orientation $\mathbf{n} \| \mathbf{H}$ prevails in the bulk in agreement with predictions of [3].

3.4. *Deformations of the tilted layers in oblique fields*

In figure 15 the influence of the field directed at the special angle calculated in [3] is shown. The deformed structure is almost uniform and finally the director becomes parallel to the external field at relatively low field strength. Hysteresis is present.

Figures 16(*a*) and 16(*b*) show examples of director

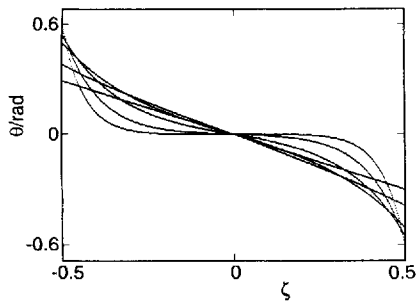

Figure 14. The director distribution in the homeotropic layer deformed by the parallel field calculated for $k_{sb} = 1{\cdot}1$ and $g = 1$. The values of U are 0, 0·8, 2·0, 3·0, 5·0 and 8·0 (in order from the lowest curvature to the highest).

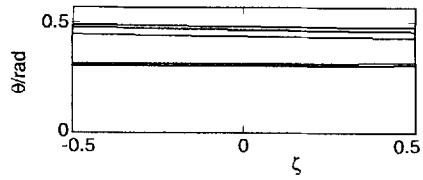

Figure 15. The director distribution of the tilted layer ($\beta = 0{\cdot}5$) in the magnetic field directed at the special angle ($\alpha = -1{\cdot}28828$) for $k_{sb} = 0{\cdot}4$ and $g = 1$. The values of U are 0·05, 0·07, 0·09, 0·07 and 0·15 (in order from the highest curve to the lowest). Two curves present for $U = 0{\cdot}07$ illustrate the existence of the hysteresis.

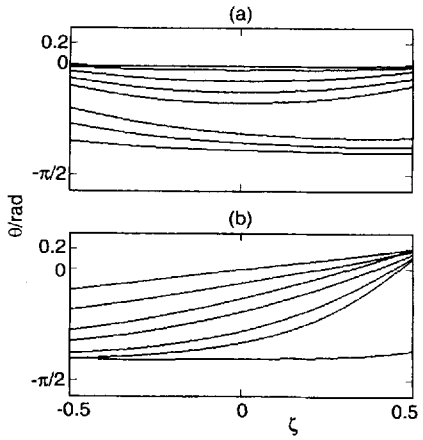

Figure 16. The director distribution in the homeotropic layer ($\beta = 0$) deformed by the oblique magnetic field ($\alpha = 0{\cdot}3$). (*a*) $k_{sb} = 0{\cdot}4$ and $g = 2$, the values of U are 0·3, 0·5, 0·8, 0·9, 1·0, 1·0, 1·1 and 1·2 (in order from the highest curve to the lowest), two curves present for $U = 1{\cdot}0$ illustrate the existence of the hysteresis; (*b*) $k_{sb} = 1{\cdot}1$ and $g = 1$, the values of U are 0, 0·5, 0·8, 1·0, 1·5, 2·0 and 3·0 (in order from the highest curve to the lowest).

profiles in the homeotropic layer deformed by the oblique field. Deformation of the uniform distribution, existing in the layer at $h = 0$ if k_{sb} is small, is almost symmetrical for low fields and discontinuously changes into asymmetrical deformation, figure 16(*a*). This change is accompanied by hysteresis. If k_{sb} is sufficiently high, then the deformation of the initial linear profile is continuous. A strong curvature characterizes the resulting distribution, figure 16(*b*). In both cases the director distributions tend to the $\mathbf{n} \| \mathbf{H}$ states in the high field.

Deformation of the tilted layer induced by the field parallel to the layer plates arises continuously. An almost symmetrical director distribution takes place for low k_{sb} and finally the state $\mathbf{n} \| \mathbf{H}$ is achieved, figure 17(*a*). In case of sufficiently high k_{sb}, the initial linear distribution is asymmetrically suppressed, figure 17(*b*).

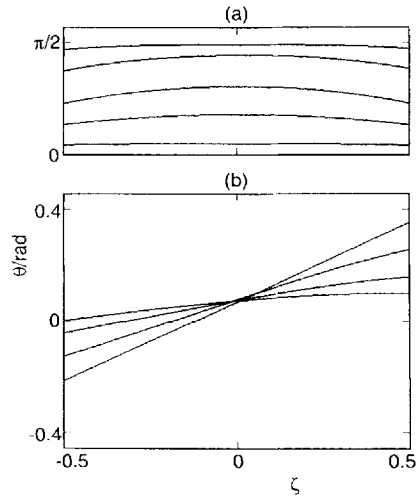

Figure 17. The director distribution in the tilted layer ($\beta = 0{\cdot}1$) deformed by the magnetic field parallel to the layer ($\alpha = 0$). (*a*) $k_{sb} = -0{\cdot}1$ and $g = 1$, the values of U are 0·5, 0·8, 1·0, 1·5 and 3·0 (in order from the lowest curve to the highest); (*b*) $k_{sb} = 1{\cdot}1$ and $g = 1$, the values of U are 0, 0·6, 0·7 and 0·8 (in order from the highest slope to the lowest).

4. Discussion

In this paper, magnetic field induced deformations of a weakly anchored nematic layer with non-zero splay-bend elastic constant k_{13}, have been analysed. According to the Pergamenshchik [2] approach applied here, the director distribution function was chosen in a form of solution of the Euler–Lagrange equation (5). The general form of this solution was adopted. Minimization of the free energy function yields the required director profile $\theta(z)$. Summarizing, the presence of $k_{sb} \neq 0$ manifests itself quantitatively and qualitatively.

In the absence of the field, the weakly anchored layer has a uniform structure $\mathbf{n} \| \mathbf{e}$ if

$$1 + g - 2k_{sb} \cos 2\beta > 0. \tag{31}$$

In the opposite case, the structure is spontaneously distorted and the director distribution is described by the linear $\theta(z)$ function.

The deformed director distribution induced by the external field is fully asymmetric in general. In some special cases this distribution can be symmetric or antisymmetric, i.e. as described by the even or odd $\delta(z)$ functions. The homeotropic layer satisfying the inequality (31) remains undeformed in a perpendicular field until some threshold strength is reached. For negative or sufficiently low positive k_{sb}, the deformation is symmetrical and arises continuously. For k_{sb} values which are sufficiently high, but still satisfy the inequality (31), the discontinuous transition to the state $\mathbf{n} \| \mathbf{H}$ occurs. For k_{sb} values which do not satisfy the inequality (31), the initial spontaneous linear deformation is suppressed by the field and disappears above another threshold. The properties of the planar layer are analogous.

In the tilted layer the deformation has no threshold, even if $\mathbf{H} \perp \mathbf{e}$. A field parallel to the surface alignment does not induce any deformation if the inequality (31) is satisfied. In the opposite case, the linear director profile is strongly distorted. A sufficiently high k_{sb} seems to favour a strong director curvature in the boundary regions in some geometries.

The phenomena which do not occur if $k_{sb} = 0$, are the most interesting. The hysteresis due to $U_2 < U_1$ shown in figure 7 is the best example of such a distinguishing effect; this could be detected in sufficiently weakly anchored (or sufficiently thin) layers, homeotropic if $k_{sb} > 0$ and planar in the opposite case. The continuously arising deformation, leading to rotation of the director if $\alpha = \beta \neq 0$, is another effect suitable for experimental verification. The zero-field spontaneous linear director distribution and its field induced deformation could be detectable if $1 + g - 2k_{sb} \cos 2\beta < 0$, i.e. if $|k_{sb}|$ is sufficiently high. The homeotropic layer would be useful if $k_{sb} > 0$ and the planar layer in the opposite case.

The procedure leading to the expressions for the thresholds (24), (27) and (29) is identical to the technique due to the method based on catastrophe theory (which was applied earlier, e.g. in [14] and [15]), and to the similar approach applied in [6] to the present problem. In this method the deformation is approximately expressed in the form of some simple trial function, which should possess the essential qualitative features of the exact solution. In normal cases, when $k_{13} = 0$ and the functional of the free energy has a minimum, there is some free choice of the trial functions which lead to qualitatively proper and identical results. However in the present situation when $k_{13} \neq 0$, various trial functions create different effective free energy functions with various minima. Some of them may yield a description of the system which may be erroneous, not only quantitatively, but also qualitatively. Therefore, the exact solution of the Euler–Lagrange equation or its close approximation should be adopted as the trial function. Here the solution is obtained from the equation derived by use of the one elastic constant approximation. Nevertheless, due to its proper qualitative features, it can be applied also in the general case. According to this assumption the threshold conditions (24), (27) and (29) can be generalized for $k_b = k_{33}/k_{11} \neq 1$

$$U_1 = \frac{g}{k_b - 2k_{sb}} \cot U_1 \tag{32}$$

$$U_2 = \frac{g}{k_b + 2k_{sb}} \coth U_2 \tag{33}$$

and

$$U_3 = -\frac{g}{k_b - 2k_{sb}} \tan U_3 \tag{34}$$

Appendix

Equation (5) is integrated once to give

$$\delta_u'^2 + \sin^2 \delta = c^2 \tag{A1}$$

where c is the integration constant. From equation (A1) one obtains

$$\frac{d\delta}{(c^2 - \sin^2 \delta)^{1/2}} = \pm du \tag{A2}$$

As both the signs lead to equivalent results, the positive sign is chosen in the following. By means of a new variable η defined by

$$\sin \delta = c \sin \eta \tag{A3}$$

the integral of equation (A2) is obtained

$$\int \frac{d\eta}{(1 - c^2 \sin^2 \eta)^{1/2}} = \int du + \text{const} \tag{A4}$$

Two cases should be considered.

(1) For $c \leqslant 1$ the integration yields

$$F(\sin \eta, c) = u + c_1 \tag{A5}$$

where $F(\sin \eta, c)$ is the incomplete elliptic integral of the first kind and c_1 is another integration constant. Equation (A5) yields the most general solution of the problem, since the constants c and c_1 are not specified. Their actual values should be found by minimizing the free energy of the layer. It is convenient to express the constant c_1 in terms of the angles β and α. For this purpose the quantity u_0 is introduced, for which the angle δ equals $\beta - \alpha$. Therefore

$$c_1 = F(\sin \eta_0, c) - u_0 \tag{A6}$$

where η_0 is a suitable value of the variable η determined by $c \sin \eta_0 = \sin(\beta - \alpha)$. As a result

$$F(\sin \eta, c) = u - u_0 + F(\sin \eta_0, c) \tag{A7}$$

The inversion of this function leads to

$$\sin \eta = \text{sn}\,[u - u_0 + F(\sin \eta_0, c), c] \tag{A8}$$

where the Jacobian elliptic function sn [11] is introduced. According to addition theorems for the Jacobian functions, this expression takes the form

$$\begin{aligned} \sin \eta = {} & [\text{sn}(u - u_0, c)\,\text{cn}(F, c)\,\text{dn}(F, c) \\ & + \text{cn}(u - u_0, c)\,\text{dn}(u - u_0, c)\,\text{sn}(F, c)] \\ & \times [1 - c^2 \text{sn}^2(u - u_0, c)\,\text{sn}^2(F, c)]^{-1} \end{aligned} \tag{A9}$$

where two other Jacobian functions cn and dn appear and the abbreviation $F = F(\sin \eta_0, c)$ is used. By means of equation (A3), one obtains finally

$$\begin{aligned} \sin \delta = {} & [\text{sn}(u - u_0, c)\cos(\beta - \alpha)(c^2 - \sin^2(\beta - \alpha))^{1/2} \\ & + \sin(\beta - \alpha)\,\text{cn}(u - u_0, c)\,\text{dn}(u - u_0, c)] \\ & \times [1 - \sin^2(\beta - \alpha)\,\text{sn}^2(u - u_0, c)]^{-1} \end{aligned} \tag{A10}$$

(2) For $c \geqslant 1$, integration of equation (A4) gives

$$\frac{1}{c} F(c \sin \eta, 1/c) = u + c_2 \tag{A11}$$

where

$$c_2 = \frac{1}{c} F\left(c \sin \eta_0, \frac{1}{c}\right) - u_0 \tag{A12}$$

The final expression, obtained in an analogous way, is

$$\begin{aligned} \sin \delta = {} & [\text{sn}(c(u - u_0), 1/c) \\ & \times \cos(\beta - \alpha)(1 - (1/c^2)\sin^2(\beta - \alpha))^{1/2} \\ & + \sin(\beta - \alpha)\,\text{cn}(c(u - u_0), 1/c)\,\text{dn}(c(u - u_0), 1/c)] \\ & \times [1 - (1/c^2)\sin^2(\beta - \alpha)\,\text{cn}^2(c(u - u_0), 1/c)]^{-1} \end{aligned} \tag{A13}$$

The constant c in the above equations can be expressed by means of the derivative δ_u' taken for $u = u_0$

$$c^2 = \delta_u'^2(u_0) + \sin^2(\alpha - \beta) \tag{A14}$$

or, if its value is smaller than 1, as the sine of the extreme angle δ_m

$$c = \sin \delta_m \tag{A15}$$

References

[1] Nehring, J., and Saupe, A., 1971, *J. chem. Phys.*, **54**, 337.
[2] Pergamenshchik, V. M., 1993, *Phys. Rev. E*, **48**, 1254.
[3] Faetti, S., 1994, *Mol. Cryst. liq. Cryst.*, **241**, 131.
[4] Barbero, G., and Strigazzi, A., 1989, *Liq. Cryst.*, **15**, 693.
[5] Faetti, S., 1993, *Liq. Cryst.*, **15**, 807.
[6] Pergamenshchik, V. M., Teixeira, P. I. C., and Sluckin, T. J., 1993, *Phys. Rev. E*, **48**, 1265.
[7] Lavrentovich, O. D., and Pergamenshchik, V. M., 1994, *Phys. Rev. Lett.*, **73**, 979.
[8] Madhusudana, N. V., and Pratibha, R., 1990, *Mol. Cryst. liq. Cryst.*, **179**, 217.
[9] Teixeira, P. I. C., Pergamenshchik, V. M., and Sluckin, T. J., 1993, *Mol. Phys.*, **80**, 1339.
[10] Stelzer, J., Longa, L., and Trebin, H.-R., 1995, *Mol. Cryst. liq. Cryst.*, **262**, 455.
[11] Abramowitz, M., and Stegun, I. A., 1972, *Handbook of Mathematical Functions with Formulas, Graphs and Mathematical Tables*, (Dover Publications), p. 569.
[12] Nehring, J., Kmetz, A. R., and Scheffer, T. J., 1976, *J. appl. Phys.*, **47**, 850.
[13] Yamada, H., 1984, *Mol. Cryst. liq. Cryst.*, **108**, 93.
[14] Derfel, G., 1988, *Liq. Cryst.*, **3**, 1411.
[15] Derfel, G., 1994, *Liq. Cryst.*, **17**, 429.